

Nuclear Magnetometry Study of Spin Dynamics in Bilayer Quantum Hall Systems

M. H. Fauzi

Department of Physics, Tohoku University, Sendai 980-8578

E-mail: fauzi@m.tohoku.ac.jp

S. Watanabe

Institute of Science and Engineering, Kanazawa University, Kanazawa, 920-1192

E-mail: wshinji@se.kanazawa-u.ac.jp

Y. Hirayama^{1,2,3}

¹Department of Physics, Tohoku University, Sendai 980-8578

²ERATO Nuclear Spin Electronics Project, Sendai 980-8578

³WPI-Advanced Institute for Materials Research, Tohoku University, Sendai 980-8577

E-mail: hirayama@m.tohoku.ac.jp

Abstract. We performed a nuclear magnetometry study on quantum Hall ferromagnet with a bilayer total filling factor of $\nu_{\text{tot}} = 2$. We found not only a rapid nuclear relaxation but also a sudden change in the nuclear spin polarization distribution after a one-second interaction with a canted antiferromagnetic phase. We discuss the possibility of observing cooperative phenomena coming from nuclear spin ensemble triggered by electrons with collective spin interactions.

Keywords: Quantum Hall Effect, Nuclear Spin, Electron Spin.

1. Introduction

The electron spins in the host GaAs semiconductor are coupled with the ensemble of nuclear spins mainly through the hyperfine (HF) interaction. The HF interaction lies at the heart of many fascinating phenomena including dynamic nuclear polarization, Knight shift, and Overhauser/Hyperfine field[1], and is of importance to development of quantum computing based on hybrid ensemble of electron-nuclear spins. The interaction has been successfully utilized to probe and characterize various electron spin cooperative phenomena in 2D systems subjected to a strong magnetic field B at low temperature, where the strong Coulomb interaction dominates the physics. Examples include evidence for the formation of a topological spin texture at a Landau level filling factor of

$\nu = 1$ as predicted by Shondhi[2] via the Knight shift[3], and nuclear spin relaxation T_1 time measurements[4]. Recently an intermediate canted antiferromagnetic state in a bilayer total filling factor $\nu_{\text{tot}} = 2$ that supports linearly dispersing Goldstone modes[5, 6] was experimentally verified by Kumada who used the Knight shift[7] and T_1 measurements[8].

A large portion of research has been devoted to the use of nuclear spins as a mere tool for studying electronic structures in quantum Hall systems, whereas little attention has been given as to how the electronic structures affect the nuclear spin. In fact, cooperative phenomena coming from an ensemble of nuclear spins induced by the HF interaction are theoretically predicted[9, 10, 11], yet to the best of our knowledge, there has been no experimental observation reported to date. One of the strongest cooperative phenomena involving electron spins appears in a bilayer canted antiferromagnetic (CAF) state as evidenced by its very short nuclear spin relaxation T_1 time[8]. Therefore, we expected there would be cooperative phenomena when an ensemble of nuclear spins interacts with the CAF state.

In this study, we developed a novel nuclear magnetometry and used it to demonstrate the possibility of collective nuclear spins relaxation due to interaction with the Goldstone mode of the CAF phase of total filling factor of $\nu_{\text{tot}} = 2$ in the quantum Hall effect. We found that the initial number of polarized nuclear spins would affect the relaxation behaviour. A pump-probe technique performed at the spin transition at the filling factor of $\nu = 2/3$ was employed to dynamically polarize the nuclear spins and probe their relaxation dynamics[4]. We analyze the position of the spin transition to estimate the hyperfine field value and its width to qualitatively discuss the homogeneity of nuclear spin polarization in the well.

2. Experimental Procedures

Experiments were carried out on high-quality 20-nm-wide bilayer GaAs quantum wells separated by a 2.2 nm $\text{Al}_{0.3}\text{Ga}_{0.8}\text{As}$ barrier. The energy separation of the symmetric and antisymmetric states, Δ_{SAS} , was 15 K at the charge balanced condition for a total electron density of $n_{\text{tot}} = 1.45 \times 10^{15} \text{ m}^{-2}$. The sample was patterned into a 30- μm -wide Hall bar, and ohmic contact pads were made with Ni/AuGe/Ni alloys annealed at 420^o C. The carrier density of the top and bottom layers (n_{f} and n_{b}) could be controlled independently from depletion to $4.0 \times 10^{15} \text{ m}^{-2}$ by applying bias voltages to the top gate made of a Ti/Au electrode deposited on top of the Hall bar and the n^+ -GaAs substrate acting as the bottom gate. At a constant magnetic field B , the filling factor was tuned by controlling the carrier density in each layer. The total filling factor $\nu_{\text{tot}} = \nu_{\text{f}} + \nu_{\text{b}}$ is the sum of the individual filling factors. All magnetotransport measurements were carried out using a quasi ac lock-in technique at 13.4 Hz and the sample was immersed in a mixture of He-4/He-3.

The key aspect of our experimental protocol are schematically displayed in Fig. 1(b)–(d). First, the carrier density in one layer (bottom layer) was set to the spin

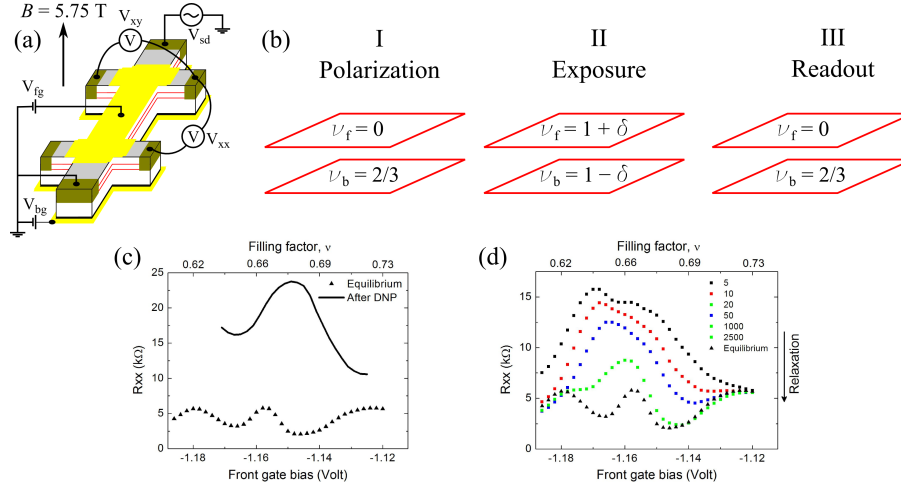


Figure 1. (a) Schematic view of device and measurement circuit. The two dimensional electron systems (2DESs) are indicated by the red lines, the top and bottom gate electrodes in yellow are used to control the electron density in the top and bottom layers, and both 2DESs share common Ohmic contacts in olive. (b) Timing sequence diagram for the nuclear magnetometry measurement. (c) Spin transition profiles before (equilibrium) and after dynamic nuclear polarization. (d) Example of nuclear spin relaxation measurement due to interaction with electrons of the bilayer: $\nu_{tot} = 2$; $\delta = 0.37$; exposure durations τ of 5 to 2500 seconds.

transition at the filling factor of $\nu = 2/3$ at constant top and bottom gate bias voltages $V_{tg} = -1.157$ V, $V_{bg} = +2.8$ V, and a constant magnetic field of $B = 5.75$ T. Subsequently, a high excitation current $I_{sd} = 60$ nA was applied for 500 sec (unless mentioned otherwise) to induce dynamic nuclear polarization (DNP). DNP provides an inhomogeneous nuclear spin polarization and results in a huge and broad spin transition peak (see section II of the supplementary material for details). Next, the carrier density was tuned in both layers to reach the quantum Hall state with $\nu_{tot} = (1 + \delta) + (1 - \delta)$ for several sets of charge imbalance variables, δ . The polarized nuclear spins then interact with electrons of the bilayer with $\nu_{tot} = 2$. We interrupted the process by temporarily restoring the filling factor to a one layer (the bottom layer) $\nu_b = 2/3$ after a given interval of time "exposure time τ " and the remaining nuclear polarization was readout by sweeping the filling factor across $\nu_b = 2/3$ ($0.61 \rightarrow 0.73$) by varying the gate bias voltages at a measurement current I_{sd} of 2 nA. The top gate voltage sweep rate was $dV_{tg}/dt \sim 3.52 \times 10^{-3} \text{ s}^{-1}$ at constant bottom gate voltage $V_{bg} = +2.8$. The sweep time from $\nu_b = 0.61$ ($V_{tg} = -1.186$, $V_{bg} = +2.8$) to $\nu_b = 0.73$ ($V_{tg} = -1.12$, $V_{bg} = +2.8$) was about 25 seconds and much faster than the nuclear spin relaxation time at $\nu = 2/3$ (> 300 seconds). The remaining polarization is a measure of nuclear spin relaxation rate due to interactions with the bilayer electrons (see Figure 1(d)).

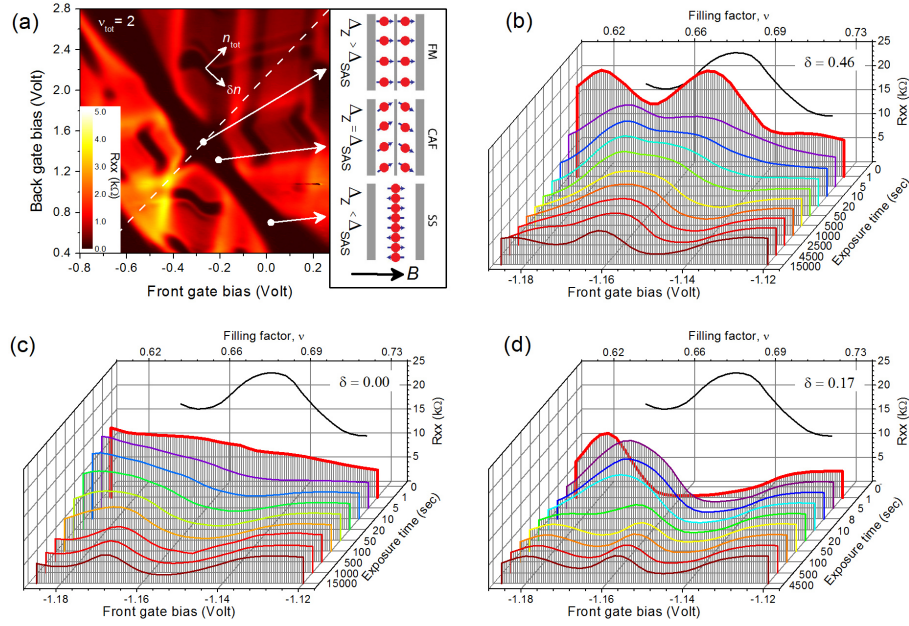


Figure 2. (a) Two dimensional plot of R_{xx} as a function of a back- and front-gate bias voltage highlighted along $\nu_{tot} = 2$ with its possible spin configurations (see the box) for 5.75 T and 50 mK. The white dashed line corresponds to the zero charge imbalance $\delta = 0$. (b)–(d) Nuclear spin relaxation process, reflected in the spin transition evolution, due to interactions with (b) the spin single (SS) phase $\delta = 0.46$, (c) the ferromagnetic (FM) phase $\delta = 0$, and (d) the canted antiferromagnetic (CAF) phase $\delta = 0.17$. The solid black line in (b)–(d) is the initial nuclear spin polarization profile taken prior to interactions with electrons of the bilayer.

3. Results and discussions

Figure 2(a) depicts a two-dimensional map of the longitudinal resistance R_{xx} highlighted along $\nu_{tot} = 2$ as a function of the top- and the bottom-gate voltages at 5.75 T and 50 mK. The phase transition between different magnetic phases along the $\nu_{tot} = 2$ was driven by altering the normalized density imbalance $\delta \equiv (\nu_t - \nu_b) / \nu_{tot}$ [12]. The quantum Hall effect was preserved from the point of no charge imbalance $\delta = 0$, where the system possessed a ferromagnetic (FM) phase, to a very large charge imbalance $\delta \approx 1$, where the spin configuration altered to a spin singlet (SS) phase when the tunneling gap Δ_{SAS} overwhelmed the Zeeman energy Δ_Z [8]. Level crossing did not take place because the transition from FM to SS phases occurred through two second-order phase transitions via an intermediate state, namely the canted antiferromagnetic (CAF) phase [5, 6].

Now let us analyze the nuclear spin relaxation due to interactions with the electrons of the bilayer $\nu_{tot} = 2$. In the SS phase depicted in Fig. 2(b), the time required to reach the equilibrium spin transition shape, T_{eq} , is very long ($T_{eq} > 4500$ sec). In addition, the way that the spin transition curve relaxes is qualitatively quite similar to our expected relaxation behavior (see supplementary Figure 2(c)). This is not surprising since the nuclear subsystem is well isolated from the electronic system, the nuclear Zeeman energy

(\sim MHz) is three order of magnitude smaller than the electron Zeeman energy (\sim GHz). It is therefore reasonable that the exchanges of energy and angular momentum are very inefficient and the SS phase cannot contribute much to the nuclear spin relaxation process. The relaxation is mainly governed by nuclear spin diffusion. For the FM phase shown in Fig. 2(c), the measured T_{eq} was ~ 500 sec, which is almost ten times faster than in the SS phase. The shape of the spin transition towards equilibrium revealed that it was rather distinct from the previous one measured in the SS phase. The curve's fall was asymmetrically; that is the resistance to the right of the peak, corresponding to $B_{\text{N}} > 0$ in Fig. 1(c), dropped more than it did on the left.

The most striking feature of the nuclear spin relaxation process was observed in the CAF phase depicted in Fig. 2(d). First of all, the T_{eq} was very short, ~ 50 sec. This indicates the appearance of electron spin fluctuations which have a high spectral density at the Larmor nuclear frequencies of Ga and As[13]; this is suggestive of the Goldstone mode as previously reported by Kumada *et al*[8]. What makes the relaxation process even more interesting is that the initial characteristics of the DNP completely disappeared one second after exposure to the CAF phase. The broad transition curve suddenly became very narrow. The resistance to the right of the peak dropped to almost zero because the downward nuclear spin polarization, which is higher in energy than the upward one, completely relaxed. The spin transition curve moved rapidly back to equilibrium by shifting back to a higher filling factor at $\nu \approx 0.66$ within $\tau \approx 50$ seconds, while its width remained narrow during the evolution. The observed response clearly indicated a sudden change in the nuclear spin polarization distribution after one second of interaction with the CAF phase. From the peak shifting and matching condition between the Zeeman and Coulomb energy scales[14], we can estimate the hyperfine field B_{N} from the remaining nuclear spin polarization one second after exposure to the CAF phase. The estimated $B_{\text{N}} = \sqrt{B_1 B_2} - B_1$ is approximately 0.66 T. It roughly corresponds to a 12.5% spatially homogeneous nuclear spin polarization, assuming that if all GaAs nuclear spins were fully polarized, the hyperfine field would be as high as 5.3 T[15]. Here, $B_2 = 4.5$ T is where the filling factor of the spin transition approximately coincided with the transition at $B_1 = 5.75$ T one second after exposure to the CAF state (see supplementary Fig. 1b). We could keep the remaining nuclear spin polarization for a significant time period (about 500 seconds) by depleting the electrons in the wells one second after exposure to the CAF phase as demonstrated in supplementary Fig. 3.

Let us elaborate on how the response changes when we decrease the current pumping time from $P = 500$ seconds. The number of polarized nuclear spins would decrease as a result of shortening the current pumping time. For all of the data presented in Fig. 3, the exposure time to the CAF phase with $\delta = 0.17$ was fixed to $\tau = 1$ second. Evidently, the response in terms of the spin transition's position and width showed a dependence on the current pumping time. The largest shift in the spin transition's position with respect to the equilibrium position ($\nu \approx 0.66$) appeared at $P = 500$ seconds, and it decayed with decreasing polarization time (see the black arrows in Fig. 3a). Interestingly as depicted in figure 3(b), its width had the opposite tendency; i.e., its value peaked at

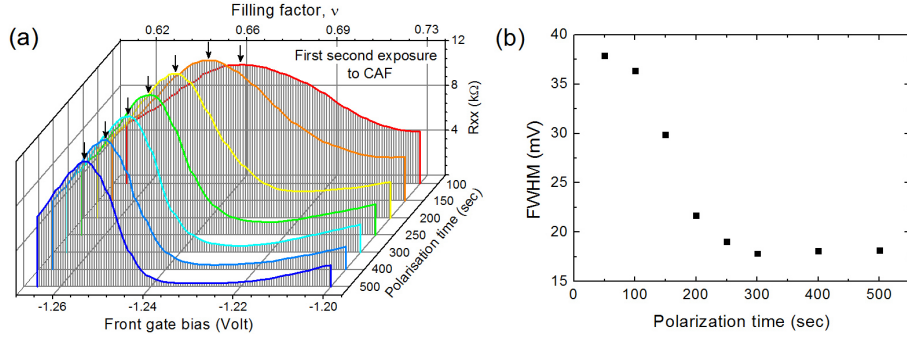


Figure 3. (a) The evolution of the spin transition after one second of exposure to the CAF phase $\delta = 0.17$ as a function of polarization time P ranging from 100 to 500 seconds. The black arrow indicates the spin transition positions which depend on the hyperfine field B_N at a fixed applied magnetic field B . (b) The full width at half maximum (FWHM) as a function of polarization time extracted from figure 3(a).

the shortest polarization time and became narrower with increasing polarization time. This suggests that for $P \leq 200$ seconds, the downward nuclear spin polarization did not completely relax.

The observed response might be the fingerprint of an emission due to a collective nuclear spin relaxation, in analogy with superradiance emission in quantum optics[16]. The possibility of observing superradiance emissions from an ensemble of nuclear spins in a magnetic field was first put forward by Bloembergen and Pound[17] and experimentally observed much later by Kiselev *et al* [18]. The motions of the inverted polarized nuclear spins can become highly correlated when the resonance circuit frequency matches the Larmor frequency of nuclei. Indeed, the present system seems to be fundamentally different than the one studied by Kiselev *et al*. The underlying interaction is an electromagnetic interaction, although the HF interaction can have a secondary effect of boosting the signal by three orders of magnitude[19]. It remains to be seen whether long-ranged Goldstone modes could potentially mimic the role played by the resonance circuit, since the modes apparently have continuous energy dispersions. However, the very short T_{eq} conspicuously suggests to us that only a certain range of frequencies close to the Larmor frequency of Ga and As nuclei are involved in the relaxation process. Recent theoretical calculations have pointed out that a superradiance-like emission could be observed from a polarized nuclear spin ensemble in systems like a nitrogen-vacancy center[10] or a single quantum dot[11]. The effect stems from the collective HF interaction between a single electron spin and surrounding nuclear spins. Whether replacing a single electron spin with a set of collective electron spins in the CAF phase could feasibly have the same effect is unclear, but it would be interesting if turned out to be true. Alternatively, as pointed out in ref [9], it might be possible that a large ensemble of polarized nuclear spins sees a common magnon field with the length scale much larger than the lattice period; in our case, this might be generated by the CAF phase, through the HF interaction. As a result, the downward nuclear spin polarization,

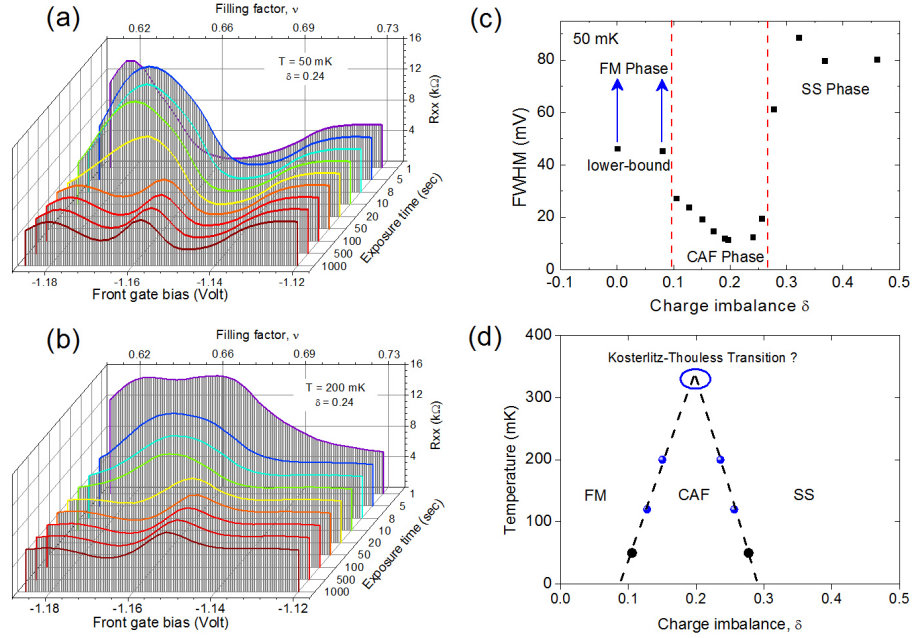


Figure 4. (a)–(b) Nuclear spin relaxation process exposed to the CAF with $\delta = 0.24$ at 50 and 200 mK. (c) Plot of FWHM a one second after exposure to the CAF states with varying δ at 50 mK. (d) Phase-diagram $\nu_{\text{tot}} = 2$ as a function of charge imbalance δ and temperature. The 50 mK data points (black dots) are extracted from figure 4(c).

which is higher in energy, would relax collectively over a short time scale.

The exact mechanism with which to produce a substantial change in the nuclear spin distribution one second after exposure to the CAF phase is still unclear. Despite this, the detailed spin transition curve $\tau = 1$ second after the exposure could help us to identify the presence of special electronic states associated with broken planar symmetry. Figure 4 illustrates the nuclear relaxation process for a certain range of temperatures and/or charge imbalances and plots the extracted FWHM. The characteristic response associated with the CAF phase for $\delta = 0.24$ disappeared upon increasing the sample temperature from 50 to 200 mK (see Fig. 4(a)–(b)). The spin transition curve noticeably became very broad for a $\tau = 1$ second exposure. This could be interpreted as possibly a straightforward signature of the transition between the CAF and SS phases. The long-ranged ordering was destroyed, resulting in incoherent coupling between the nuclear and electron spins. We note that the difference in the final transition position at equilibrium ($\tau = 1000$ seconds) between the 50 and 200 mK data sets is due to a decrease in the thermal equilibrium nuclear spin polarization of about 3.2% at $B = 5.75$ T.

Depicted in Fig. 4(c) is the FWHMs extracted from a set of δ values at 50 mK. All data were extracted from $\tau = 1$ second responses except for those $\delta < 0.1$, which are from $\tau = 20$ seconds responses and can be used as lower bounds for the $\tau = 1$ second values. The transitions between the different electron spin phases are clearly marked by sudden changes in the width of the transition curve at $\delta = 0.104$ and $\delta = 0.276$

(indicated by the vertical red dashed lines). The clear transition helped us to construct the thermodynamic phase-diagram depicted in Fig. 4(d). Although the data were limited to the range of 50 to 200 mK, we can see that the area at which the CAF state was expected to occur shrank as the sample temperature was raised. We estimated that the CAF state would completely disappear above 300 mK by extrapolating the data linearly to the point where both lines converge (blue oval). For a quantum Hall state with easy-plane quantum ferromagnets, this point is associated with Kosterlitz-Thouless (KT) transition temperature[20]. The estimated $T_{\text{KT}} \sim 300$ mK from our experiment is lower than the theoretical prediction $T_{\text{KT}} = 1$ K[6], but in agreement with the previously estimated T_{KT} deduced from resistively detected T_1 measurements[8]. We believe that this discrepancy was due to disorder that might significantly lower the critical temperature T_{KT} [21].

In summary, we uncovered an unusual nuclear spin relaxation process due to interaction with the CAF phase by measuring the full profile of the $\nu = 2/3$ spin transition. We observed that only when the current pumping time was greater than the 200 seconds did the downward nuclear spin polarization completely relax after a one second interaction with the CAF phase. This could indicate the possibility of a collective relaxation from a large ensemble of polarized nuclear spins. Our measurement scheme and analysis of the FWHM of the spin transition $\nu = 2/3$ could be used to identify the transition between different phases existing at $\nu_{\text{tot}} = 2$ and draw a $T - \delta$ diagram of the CAF phase.

Acknowledgements. We thank K. Muraki of NTT Basic Research Lab for providing us the bilayer wafer. We thank Y. Hama, K. Akiba, S. Miyamoto, K. Hashimoto, and T. Hatano for fruitful discussions. We gratefully acknowledged the partial financial support by the Tohoku University GCOE program.

References

- [1] A. Abragam. *The Principle of Nuclear Magnetism*, Oxford University Press, Oxford, (1961).
- [2] S. L. Sondhi *et al.*, *Phys. Rev. B* **47**, 16419 (1993).
- [3] S. E. Barrett *et al.*, *Phys. Rev. Lett.* **74**, 5112 (1995).
- [4] K. Hashimoto *et al.*, *Phys. Rev. Lett.* **88**, 176601 (2002).
- [5] S. Das Sarma, S. Sachdev, and L. Zheng, *Phys. Rev. Lett.* **79**, 917 (1997).
- [6] S. Das Sarma, S. Sachdev, and L. Zheng, *Phys. Rev. B* **58**, 4672 (1998).
- [7] N. Kumada, K. Muraki, and Y. Hirayama, *Phys. Rev. Lett.* **99**, 076805 (2007).
- [8] N. Kumada, K. Muraki, and Y. Hirayama, *Science* **313**, 329 (2006).
- [9] V. F. Los, *Hyperfine Interactions* **59**, 357 (1990).
- [10] E. M. Kessler *et al.*, *Phys. Rev. Lett.* **104**, 143601 (2010).
- [11] M. J. A. Schuetz *et al.*, *Phys. Rev. B* **86**, 085322 (2012).
- [12] L. Brey, E. Demler, and S. Das Sarma, *Phys. Rev. Lett.* **83**, 168 (1999).
- [13] S. M. Girvin, *arXiv:cond-mat/9907002v1* (1999).
- [14] K. Akiba *et al.*, *Appl. Phys. Lett.* **99**, 112106 (2011).
- [15] D. Paget, G. Lampel, B. Sapoval, and V. I. Safarov, *Phys. Rev. B* **15**, 5780 (1977).
- [16] R. H. Dicke, *Phys. Rev.* **93**, 99 (1954).
- [17] N. Bloembergen and R.V. Pound, *Phys. Rev.* **95**, 8 (1954).

- [18] J. F. Kiselev *et al.*, *Mod. Phys. Lett. B* **1**, 409 (1988).
- [19] V. I. Yukalov, M. G. Cottam, and M. R. Singh, *Phys. Rev. B* **60**, 1227 (1999).
- [20] J. M. Kosterlitz, and D. J. Thouless, *J. Phys. C* **6**, 1181 (1973).
- [21] J. Sun, G. Murthy, H. A. Fertig, and N. Bray-Ali, *Phys. Rev. B* **81**, 195314 (2010).

Supplementary Materials

M. H. Fauzi

Department of Physics, Tohoku University, Sendai 980-8578

E-mail: fauzi@m.tohoku.ac.jp

S. Watanabe

Institute of Science and Engineering, Kanazawa University, Kanazawa, 920-1192

E-mail: wshinji@se.kanazawa-u.ac.jp

Y. Hirayama^{1,2,3}

¹Department of Physics, Tohoku University, Sendai 980-8578

²ERATO Nuclear Spin Electronics Project, Sendai 980-8578

³WPI-Advanced Institute for Materials Research, Tohoku University, Sendai 980-8577

E-mail: hirayama@m.tohoku.ac.jp

PACS numbers: 00.00, 20.00, 42.10

Keywords: Quantum Hall effect, Nuclear spin, Electron spin.

1. Spin Transition at $\nu = 2/3$

In the composite fermion (CF) model, the filling factor $\nu = 2/3$ corresponds to integer filling factor $\nu_{\text{CF}} = 2$ of CF, the two CF Landau levels are fully occupied below the Fermi energy E_{F} . The CF particle at $\nu = 2/3$ comprises of one electron and two magnetic flux quanta[1]. Consequently, the CFs experience a reduced magnetic field, which in mean field approximation, is given by

$$B_{\text{eff}} = B(1 - 2\nu) \quad (1)$$

therefore the effective magnetic field experienced by the CFs at $\nu = 2/3$ is $B_{\text{eff}} = -B/3$. Similar to the normal Landau level, the CFs energy spectrum is also quantized into a series CF Landau levels. Each CF Landau levels is separated by

$$\hbar\omega_{\text{CF}} = \frac{e\hbar}{m_{\text{CF}}} \frac{B}{3} \quad (2)$$

here $m_{\text{CF}} \equiv \alpha\sqrt{B}m_e$ is the composite fermion effective mass [2]. Due to the Zeeman effect, each CF Landau levels further splits into two spin sublevels separated by $E_Z = |g^*|\mu_B B$. The levels $(0, \downarrow)$ and $(1, \uparrow)$ can cross each other at certain range of

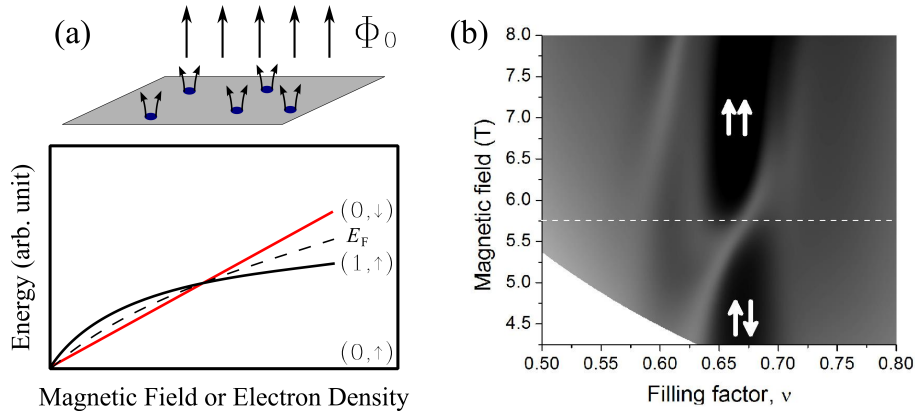


Figure 1. (a) Composite fermion Landau level energy diagram at the filling fraction $\nu = 2/3$. The state is indicated by the bracket (n, m) , n corresponds to the number of Landau level $n = 0, 1, 2, \dots$ and $m = \uparrow, \downarrow$ corresponds to the spin state $\pm 1/2$. (b) Two dimensional map of R_{xx} around filling fraction $\nu = 2/3$. The spin configurations of each ground states are indicated by the white arrows. Dark (Bright) color has a low (high) intensity. We fixed the magnetic field throughout the experiment at 5.75 T indicated by a horizontal white dashed line.

magnetic field B when the Zeeman energy equals to the CF cyclotron energy gap (see Fig. 1a). The electronic system at the transition experiences a first-order spin-phase transition from a spin-unpolarized ($\uparrow\downarrow$) to a spin-polarized ($\uparrow\uparrow$) ground state (see Fig. 1b) as the magnetic field further increases above a critical field B_t . Recently an indication of ferromagnetic-like state formation—i.e. two different electron spin domains ($\uparrow\downarrow$ and $\uparrow\uparrow$) separated by domain walls—at the transition point has been uncovered through magnetotransport experiments[3, 4], NMR spectroscopy[5], as well as from microscopic standpoint[6]. The level crossing is given by the following equation

$$|g^*|\mu_B B = \frac{e\hbar}{m_{CF}} B |1 - 2\nu| \quad (3)$$

and hence

$$B_t = 4 \left(\frac{1 - 2\nu}{\alpha |g^*|} \right)^2 \quad (4)$$

2. Detection of Nuclear Spin Polarization

In GaAs, which has s type conduction band, the interaction between electron and nuclear spin is mainly through the contact hyperfine interaction. An ensemble of nuclear spin polarization collectively generates an effective magnetic field (hyperfine field B_N) on the electron spin. This hyperfine field modifies directly the electronic Zeeman energy

$$E_Z = |g^*|\mu_B (B + B_N) \quad (5)$$

here $B_N = A \langle I_Z \rangle / g^* \mu_B$ has an effect of reducing or increasing the Zeeman energy. Since $g^* = -0.44$ has a negative value, the upward nuclear spin polarization ($\langle +I_Z \rangle$) ($B_N < 0$) has an effect of reducing the Zeeman energy and vice versa.

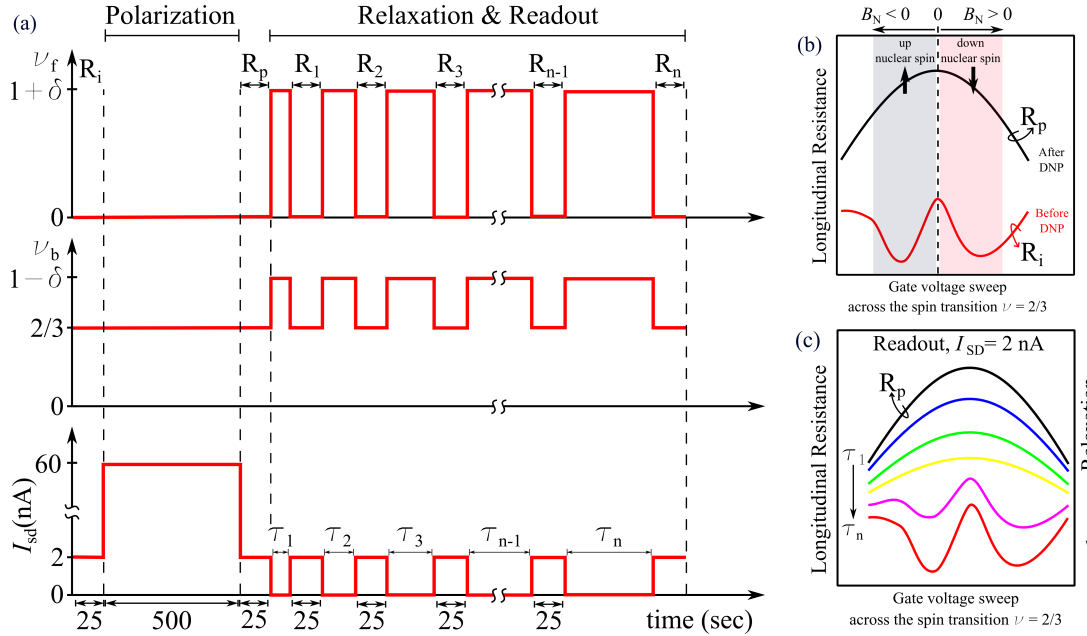


Figure 2. (a) Schematic illustration of the timing sequence of experimental procedure. (b) The schematic profile of the spin transition before and after DNP. (c) The expected nuclear relaxation process is schematically shown.

At the spin transition, the energy mismatches between electron and nuclear spin is reduced which allows them to couple effectively. The nuclear spin can be dynamically polarized effectively because when the electron spin scatters across two domains, it does so by flipping nuclear spin around the domain boundaries to preserve total angular momentum. In addition, the level crossing equation also gets modified by the presence of the hyperfine field

$$|g^*|\mu_B(B + B_N) = \frac{e\hbar}{m_{CF}}B|1 - 2\nu| \quad (6)$$

A tiny amount of the nuclear polarization down to 2% thermal equilibrium nuclear polarization can be detected sensitively by the spin transition[7].

Details of the experimental procedure timing to study nuclear-electron spin dynamics are schematically depicted in figure 2(a), constituting of polarization, relaxation, and readout schemes. The technique lies at the heart of timing control of the carrier density in each layers and switching on and off the excitation current.

The profiles of the spin transition before and after DNP are schematically depicted in figure 2(b). The huge electrical current flips electron spins at domain wall boundaries and corresponding nuclear spins leading to spin polarization in the quantum well. The upward and downward nuclear spin polarization contributes to the broadening and huge enhancement of the spin transition profile. The resistant enhancement to the left of the peak ($B_N < 0$) is attributed to the upward nuclear spin polarization $\langle +I_Z \rangle$ and the right one ($B_N > 0$) is attributed to the $\langle -I_Z \rangle$. The expected response of nuclear spin

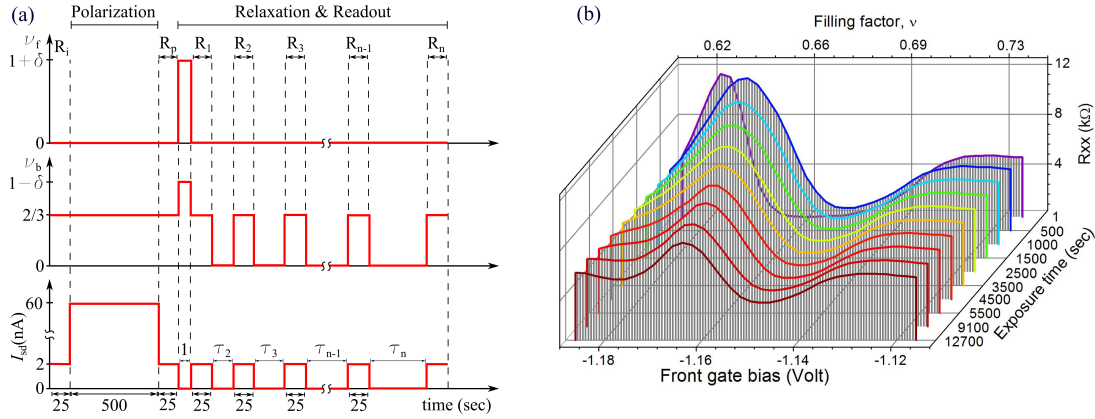


Figure 3. (a) Extended experimental protocol and timing sequence to study redistribution of nuclear spin polarization due to interaction with the CAF state. (b) The spin transition profile due to interaction with the CAF state for $\tau = 1$ second and no electrons for $\tau > 500$ seconds.

relaxation process, in the simple consideration where the upward and downward nuclear spins relax equally at the same rate, is depicted in Fig. 2(c). The broadened and huge spin transition right after DNP gradually relaxes back towards its equilibrium shape.

3. Further Evidence of Sudden Redistribution of Nuclear Magnetization

To get further insight into the redistribution of the ensemble of nuclear spins due to interaction with the CAF state for $\tau = 1$ second, we carried out the experimental procedure described in figure 3(a). The procedure is similar to figure 2(a) except right after the one second exposure to the CAF, we depleted the carrier density in each layers by applying $V_{fg} = -1.1$ Volt and $V_{bg} = -0.5$ Volt. The evolution of the transition curve presented in Figure 3(b) followed much the same way with the CAF state, however, with a longer time scale of about two order of magnitude slower to reach equilibrium compared to the evolution time scale of Figure 2(d) in the main paper. The spin transition relocated very slowly to a higher filling factor with the width characteristic apparently was not altered significantly i.e the peak remained narrow during the relaxation.

- [1] Jain, J. K. *Phys. Today* **53**(4), 39 (2000).
- [2] I. V. Kukushkin, K. von Klitzing, & K. Eberl. *Phys. Rev. Lett.* **82**, 3665 (1999)..
- [3] J. Eom, *et al. Science* **289**, 2320 (2000).
- [4] J. H. Smet, R. A. Deutschmann, W. Wegscheider, G. Abstreiter, & K. von Klitzing. *Phys. Rev. Lett.* **86**, 2412 (2006).
- [5] O. Stern, *et al. Phys. Rev. B* **70**, 075318 (2004).
- [6] B. Verdene, *et al. Nat. Phys.* **3**, 392 (2007).
- [7] M. H. Fauzi *et al. J. Korean Phys. Soc.* **60**, 1676 (2012).